

Performance of Offshore Steel Jacket Platforms under Near-source Ground Motion Type Pulses

M. Zeinoddini*, S. A. Hossini, H. Matin Nikoo

Department of Civil Engineering, K. N. Toosi University of Technology, Tehran, Iran

Abstract

Behaviour of jacket type offshore structures under ordinary ground excitations has already been addressed by a number of researchers. However, their performance under near-source ground excitations has not been particularly addressed in the literature. Records from recent earthquakes, such as the Kobe Japan (1995) and Chi-Chi Taiwan (1999), have revealed that the dynamic excitations in near-source are dominated by a large, narrow band and long period pulse caused by rupture directivity effects. Failure and sever damages were reported to occur in specific bridges, quay walls and multistory buildings near to the shaking fault. The dynamic characteristics of the damaged structures were close to the traits of the rupture directivity and fling pulses. This paper deals with the behaviour of jacket offshore structures under near-source strong ground excitations. A finite element approach has been chosen for this study. The numerical model has first been verified against available experimental data on tubular frames from other researchers. The verified model has then been used to examine the response of the jacket platform models, typical to those in the Persian Gulf, under harmonic, near-source and far-source excitations. To get an insight into both the pre and post failure zones of the structure response, an Incremental Dynamic Analysis (IDA) method has been employed. In general, it has been found that with some jacket models the near-source excitations appear quite critical as compared with those from the corresponding far-sources. Conversely, with other some models, the far-source excitations have been found to be more unfavorable.

Keywords: Offshore Steel Platforms, Near-field Earthquakes, Incremental Dynamic Analysis (IDA)

***Author for Correspondence** E-mail: zeinoddini@kntu.ac.ir

INTRODUCTION

Offshore platforms are usually located in the hostile environment, so dynamic loads including wind, wave and current dominate the design of offshore structures. In seismically active offshore zones, earthquake excitations have also to be considered in the design of the fixed platforms. A number of researchers have already addressed behaviour of jacket type offshore structures under ordinary ground excitations [1–4].

Over the past few years, there has been a growing recognition that near-source ground excitations are different from ordinary ground strong excitations in several significant ways. In fact, the associated high PGA and the pulse-like velocity waveform of the near-source ground excitation will cause much more

severe damages to structures with short and long natural periods, respectively. These near-source effects were first noticed in the 1952 Kern County, California earthquake [5], but serious concerns were raised following the Northridge, California (1994), and Hyogo-ken Nanbu (Kobe 1995) Japan, earthquakes. Relatively extensive researches have then been carried out to evaluate the so-called "near-source", "near-field" or "near-fault" earthquake effects on different types of structures such as bridges [6], dams [7], low and middle-rise buildings [8], multistory buildings [9] and gravity quay-wall structures [10]. Several previous studies have demonstrated that near-source ground excitations are more critical than the far-source earthquakes [7, 11]. The near-source effects have also then been incorporated in some

design codes, for example; GB50011 [12]. This paper deals with the performance of jacket offshore structures under near-source strong ground excitations. A finite element approach has been chosen for this study. The numerical model has first been verified against available experimental data on tubular frames from other researchers. The verified model has then been used to examine the response of the jacket platform models typical to those in the Persian Gulf under harmonic, near-source and far-source excitations. A dynamic nonlinear direct integration analysis method has been used.

METHODOLOGY

Characteristics of Near-Source Ground Excitations

Near-source strong ground excitations differ from those far to the fault in many respects such as the period of earthquake continuity, peak ground acceleration, velocity and displacement, rupture directivity, fling step and pulse properties. Values from 15km [13] up to 60km [14] were mentioned for the near-source zone radius. The near-source ground excitation is complicated by the irregular distribution of fault slip caused by non-uniform and asymmetric distribution of geologic rigidities surrounding the fault, non-uniform distribution of stress on the fault, and complex nonlinear processes that accompany faulting [9].

One of the primary factors affecting excitations in the near-source region is the direction in which rupture progresses from the hypocenter along the zone of rupture. "Directivity" refers to the direction of rupture propagation (see Figure 1) as, opposed to the direction of ground displacement [15]. A site may be classified after an earthquake as demonstrating forward, reverse, or neutral directivity effects. If the rupture propagates toward the site and the angle between the fault and the direction from the hypocenter to the site is reasonably small, the site is likely to demonstrate forward directivity (Figure 1). If the rupture propagates away from the site, it will likely demonstrate reverse directivity. If the site is more or less perpendicular to the fault from the hypocenter it will likely demonstrate neutral directivity [16].

Rupture often propagates at a velocity close to the velocity of shear wave radiation, so energy is accumulated in front of the propagating rupture. This is essentially the same principle as a sonic boom. It can be seen in Figure 2 that the seismic energy from each fault segment arrives at site A at almost the same time, resulting in a relatively short duration record containing large amplitudes [16]. Site B, however, experiences the seismic energy distributed over a much larger period, resulting in a longer duration record with lower amplitudes. Therefore, the excitation with a forward directivity is characterized by large-amplitude pulses in the velocity and displacement time histories. On the other hand, the excitation recorded in the backward directivity does not show pulse characteristic [15]. These can be noticed for example in Figure 3, which shows two records obtained in near-source areas during the 1992 Landers earthquake [17]. Both figures illustrate the time history of ground excitation for the fault normal component (most of the largest pulses occur in the fault-normal direction). The peak value of the velocity in Figure 3a is around three times bigger than in Figure 3b and, comparatively, the maximum values of acceleration and displacement for forward directivity are bigger than for backward directivity.

So, near-source ground excitations often contain strong coherent dynamic long period pulses and permanent ground displacements. The dynamic excitations are dominated by a large long period pulse of motion that occurs on the horizontal component perpendicular to the strike of the fault, caused by rupture directivity effects. Near-source recordings from recent earthquakes indicate that this pulse is a narrow band pulse whose period increases with magnitude [6]. The static ground displacements in near-source ground excitations, caused by the relative movement of the two sides of the fault on which the earthquake occurs, is the source for another type of pulse namely fling step pulse.

In fact, the phrase "directivity effects" usually refers to "forward directivity effects", as this case result in ground excitations that are more critical to engineered structures and is expressed in the forward directivity region as a

large velocity pulse [16]. This velocity pulse can also be identified in some other near-

source earthquake records [18] (see Figure 4).

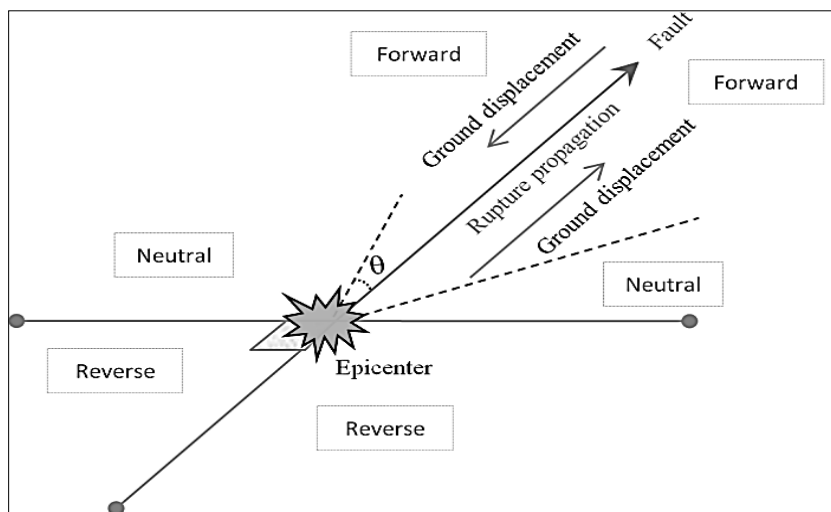


Fig. 1: Forward, Reverse, or Neutral Directivity Effects, θ is Reasonably Small.

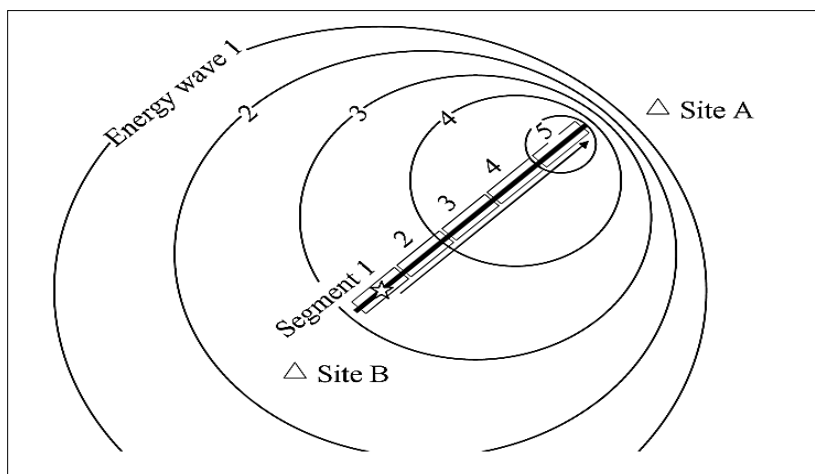


Fig. 2: Accumulation of Seismic Energy [16].

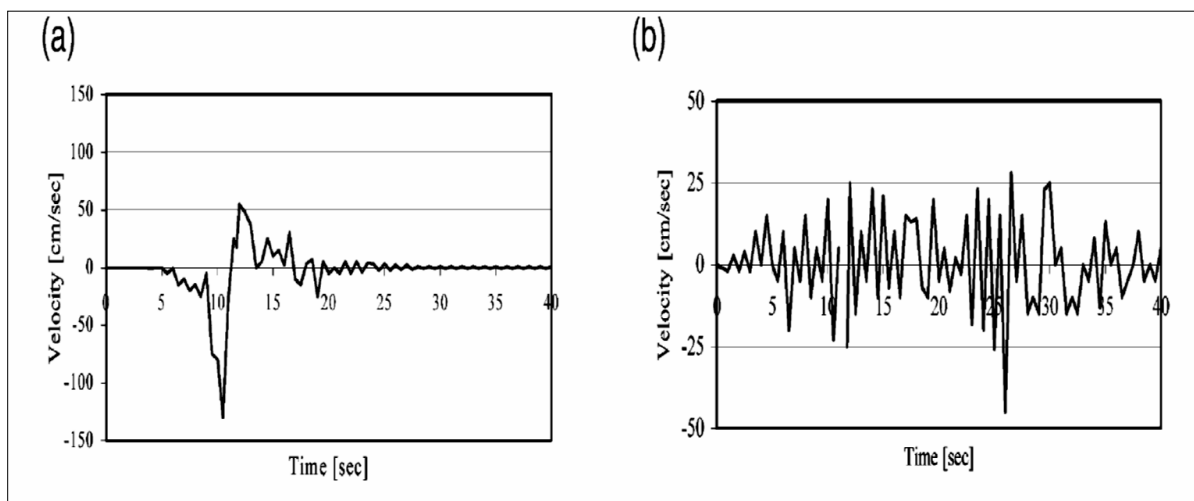


Fig. 3: Ground Velocity Time History of Fault-Normal Component: a) with Forward Directivity, b) with Backward Directivity [17].

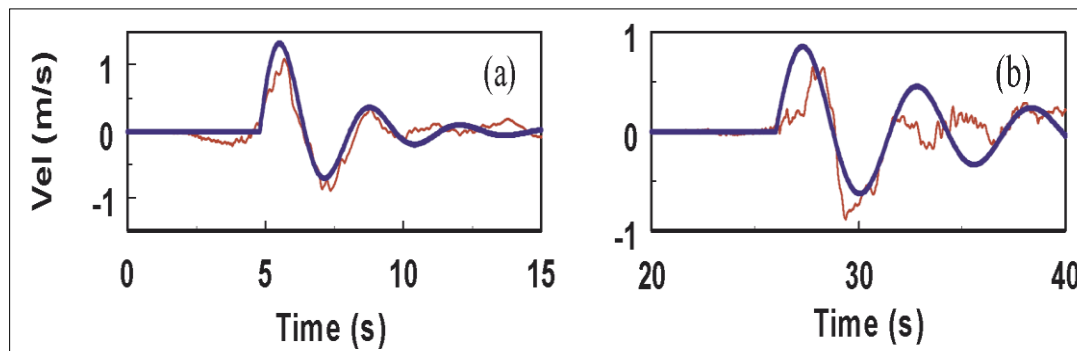


Fig. 4: Velocity Time History of Two Typical Near-Source Ground Excitations with Distinct Pulses in the Velocity Time History; a) The 1979 Imperial Valley Ground Excitation Record During a M6.5 strike-Slip Earthquake, b) The 1999 Chi-Chi Earthquake [18].

JACKET PLATFORM MODELS

In the current study, two six-leg jacket platforms currently operating in the South Pars gas field in the Persian Gulf in 72.5m and 38m water depths were examined against incrementally scaled up far and near-source

earthquake intensities (see Figures 5 and 6). The through leg piles in each platform have a penetration depth of 55m and 42m, respectively, below the seabed. Some general information about these two platforms and some views are given in Tables 1 and 2.

Table 1: General Information of the Platforms.

Component	P3D Jacket	SP2 Jacket
Topside weight	417ton	5450ton
Yield stress for the steel material	244MPa	355MPa
Water depth	38m	72.5m
Jacket height from the seafloor	44m	78.5m
Leg number	6	6
Pile penetration depth	42m	55m
Pile dimension	900×25mm	1830×35mm

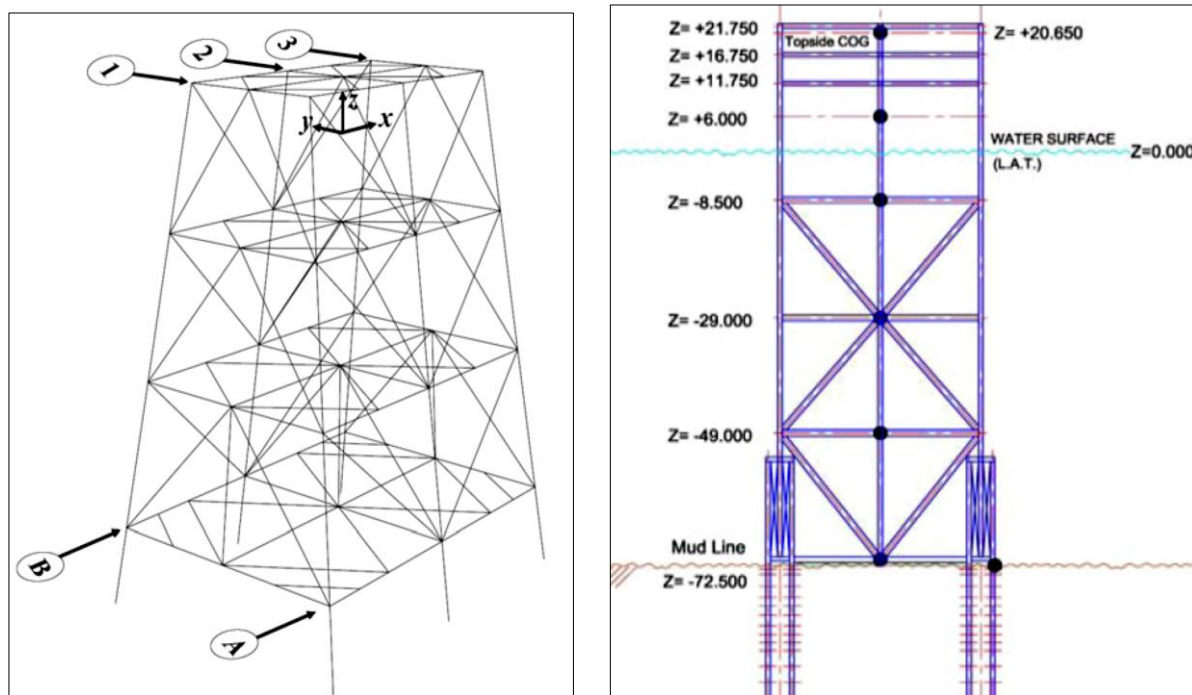


Fig. 5a: Three Dimensional View of Platform P3D (left) and Side View of Platform SP2 (right).

Table 2: Sections Dimensions in Platform P3D.

Section ID	Diameter (in)	Thickness (in)	Section ID	Diameter (in)	Thickness (in)
1	16	0.375	8	20	0.75
2	20	0.375	9	20	0.375
3	12.75	0.375	10	24	0.375
4	20	1	11	16	0.5
5	18	0.375	12	16	0.75
6	40	1	13	18	0.75
7	39	0.5	Piles	36	1

In the seismically active areas, platform response to intense ground excitations usually involves inelastic behavior. Time domain, nonlinear, inelastic and dynamic analysis becomes necessary to demonstrate the sufficient structural system redundancy such that the load redistribution and inelastic deformation will occur to prevent offshore structural collapse or the abrupt changes in stiffness in the vertical configuration of the offshore structure [3].

The numerical analysis has been carried out using a commercial nonlinear finite element program, designed specifically for advanced structural analysis [19]. The platform model includes the topside, jacket, foundation piles and soil elements. The analysis is performed using two and three dimensional structural models accounting for nonlinear soil-pile

interactions. As the input excitations are going to be incrementally intensified up to the point of dynamic instability in the system (see next Sections), some of the structural elements are expected to develop the post-yield or post-buckling and nonlinear cyclic hysteretic behavior. The inelastic behavior of the structure has been modeled utilizing an advanced nonlinear inelastic FEM buckling analysis considering material and large deformations nonlinearities. Up to 20 nonlinear beam-column elements (type PIPE31) have been used for individual jacket members (see Figure 5). The connections have been considered to be rigid. No structural elements have been assigned for appurtenances such as straight conductors, J-tubes, risers and casings, but they have been introduced to the jacket model through extra point loads and lumped masses.

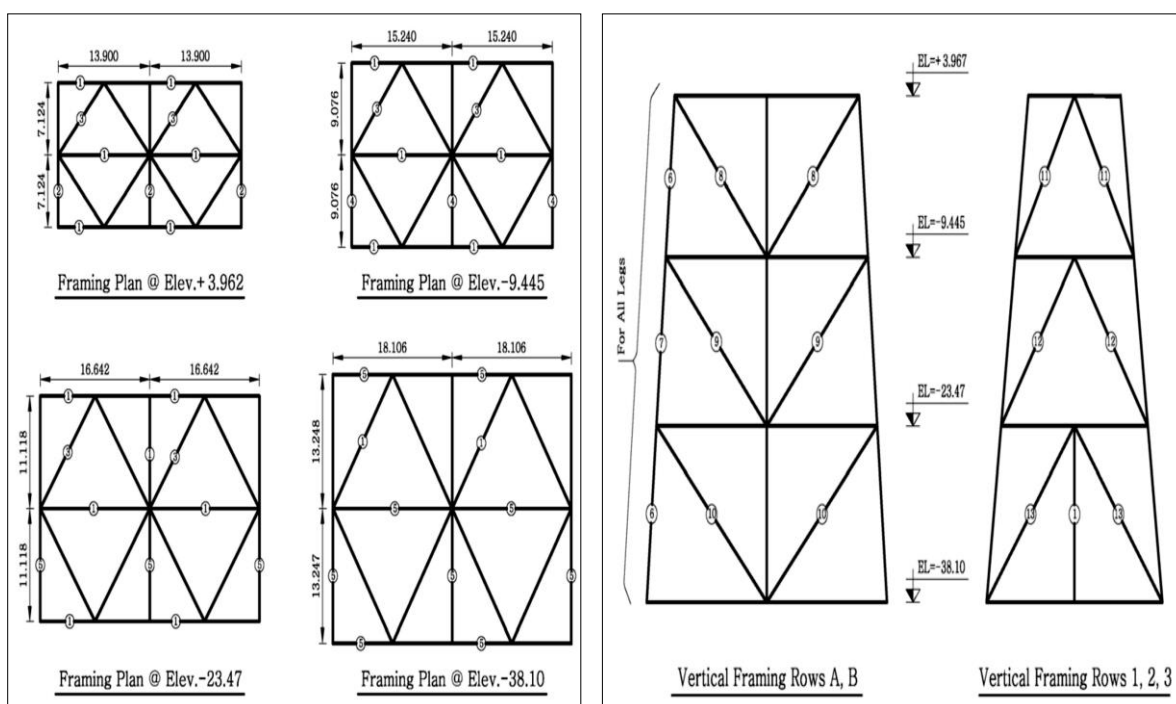


Fig. 5b: Platform P3D; Plan View at Different Elevations (left) and Side Views (right).

The lateral soil resistance has been modeled by a set of springs normal to the axis of piles having a nonlinear behavior described by so-called “p-y” curves (see Figure 6). The tangent soil pile friction has been modeled by nonlinear springs paralleled to the axis of the pile and having nonlinear behavior described by so-called “t-z” curves. The end-bearing has been modeled by a no-tension spring located at the tip of the pile and acting along the axis of the pile and having nonlinear behavior described by so-called “q-z” curves.

The platform deck has been modeled using rigid beam elements. Distributed masses along the topside horizontal members of the numerical model represent the deck floor masses and their gravity loads.

An implicit step-by-step direct integration method with a Newmark integration scheme has been employed to study the models under

sever excitations. The equilibrium of the system is achieved using an iterative solution strategy of modified Newton-Raphson method. Direct integration method is probably the most powerful technique for solving the nonlinear equations of motion in finite element dynamic analysis. The iterative equations in the dynamic nonlinear analysis using implicit time integration are of the same form as the equations that are considered in the static nonlinear analysis, except that both the coefficient matrix and the nodal force vector contain contributions from the inertia of the system [20,21].

Damping ratios of 5 and 0.5 percent have been considered for the first and second modes of vibration, respectively. Rayleigh proportional damping [20,21] has been adopted in the space frame model to account for material plus hydrodynamic damping.

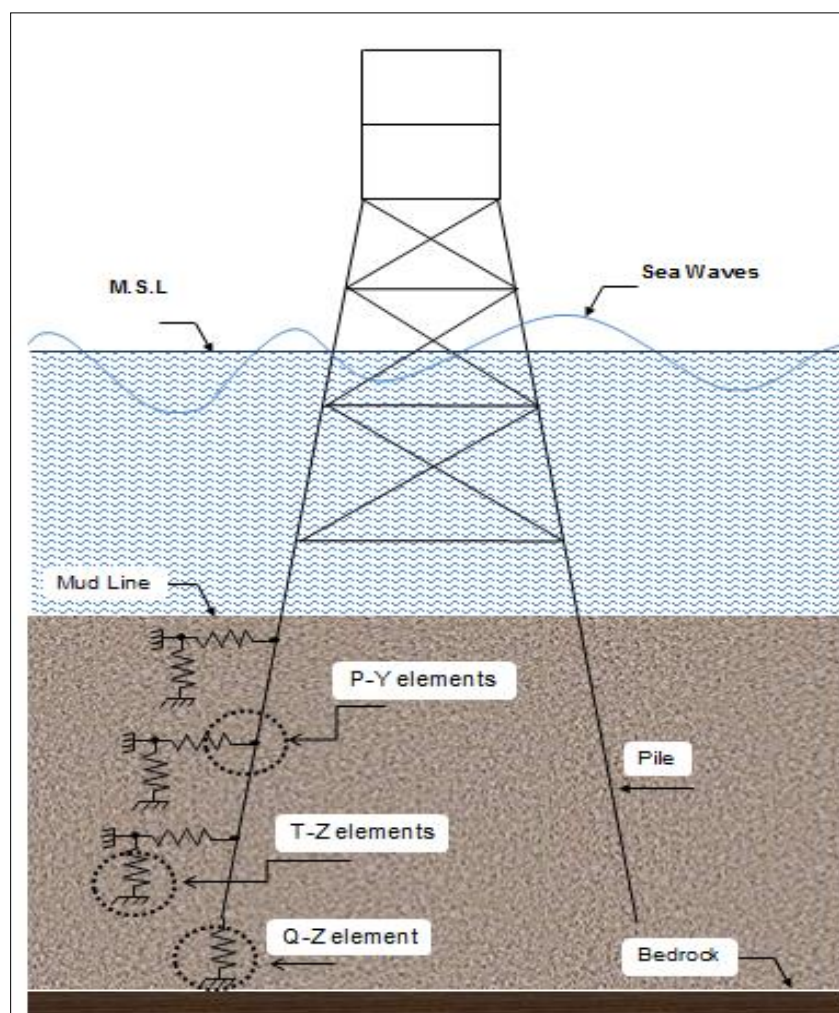


Fig. 6: Modeling of Soil-Pile Interaction.

It is assumed that the jacket structure is not concurrently becoming subject to the earthquake, sea waves and currents. Consequently, the earthquake only causes linear perturbations of water particles around their original positions. So, the undisturbed fluid pressure, or Froude-Krylov force has not been included in the analysis as this type of force is related to the absolute acceleration of the fluid body. An added mass coefficient of $C_A=1$ has been considered for the submerged tubular elements to account for the disturbed fluid pressure or inertia reactions due to relative acceleration of the body with the surrounding fluid. The marine growth mass and its associated added mass have been included in the total mass of the jacket members. A frequency analysis of the model showed the first natural period of the structure to be 1.49s.

VALIDATION OF THE NUMERICAL MODEL

The experimental data, which has been used for benchmarking the non-linear finite element models of tubular frames, emanate from the Phase I Frames Test Programme carried out in the UK. The programme was conducted by Billington Osborne-Moss Engineering Limited (BOMEL) as part of a joint industry programme with the object of providing test data on the collapse behaviour of jacket structures and in addition, to develop calibrated software for the non-linear push over analysis of framed structures [22].

The Phase I Frames Test Programme consisted of testing four, two bays, X-braced frames. These tubular frames (see Figure 7) were tested to collapse in a controlled manner, and provided a new and important insight into the role of redundancy and particularly tubular joint failures within a frame [22]. Nichols et al. have published the results of this benchmarking exercise [23].

Figure 8 shows the horizontal load-displacement curves from the experimental results and in addition from the two numerical models. The frame has been subjected to a push over horizontal load at its top. As it can be seen, there has been good agreement between the test and the numerical results.

Buckling of the compression brace at the top half of the upper bay was reported to have caused failure in the test specimen. The same phenomenon has been observed to occur in the simulations. The ultimate lateral capacity of the frame tested was 920kN. The lateral capacity predicted by both the numerical models has been found to be 932kN. It is acknowledged that the experiment referenced above and the associated numerical simulations are of a quasi-static nature. In the absence of data from proper related large-scale experiments, however, this verification attempt may provide some basis to justify the competence of the numerical model employed for a dynamic simulation job.

GROUND EXCITATION ACCELEROGRAMS

Perhaps one of the limitations to the study of near-source effects is the relatively limited amount of relevant seismic recordings from the near-source region (Cox and Ashford, 2002). Until 1994 and 1995, almost all recorded ground excitations were of earthquakes too far away to exhibit a large velocity directivity pulse. Before this time, those few stations lucky enough to be in the right place at the right time to record a pulse were not usually capable of recording such excessive ground excitations. The recent earthquakes in Turkey (August 17, 1999, Kocaeli) and Taiwan (September 20, 1999, Chi-Chi) have significantly increased the amount of data available in the near-source and forward directivity region.

For the current study, the near-source inputs from three accelerograms listed below have been used:

- Dayhook accelerogram recorded during the 1978 Tabas, Iran earthquake of magnitude M_w of 7.4,
- Kobe (JMA) accelerogram recorded during the 1995 Hyogo-ken Nanbu (Kobe) Earthquake of magnitude M_w of 6.9,
- Sepulveda VA Hospital accelerogram recorded during the 1994 Northridge Earthquake of magnitude M_w of 6.7.

In addition to these near-source accelerograms, far-source records from the same earthquakes, as listed in Table 3, are also available and have

Table 3: Some Data about the near and Far-Source Records used in the Current Study.

Accelerogram	PGA (g)	Distance from the fault (km)	Dominant period (s)
Kobe (1995)	0.035	157	4.31
Kobe (1995)	0.44	1.2	0.47
Northridge (1994)	0.04	117	0.27
Northridge (1994)	0.457	9	0.14
Tabas (1978)	0.025	199	1.58
Tabas (1978)	0.733	5	0.18

INCREMENTAL DYNAMIC ANALYSIS (IDA)

The IDA approach is a powerful method for analyzing the behavior of structures under severe dynamic loads. This approach was used to numerically evaluate the failure behavior of axially compressed steel tubes subjected to dynamic lateral impacts [24]. The lateral impact was incrementally intensified until unbounded responses were developed (see Figure 10). It was concluded that, with a direct integration incremental dynamic approach, an unbounded response indicates the propagation of dynamic instability in the system.

IDA was further developed to forecast the seismic demand of structures subjected to incrementally scaled ground excitations records [26]. In this view, IDA is the dynamic equivalent to a familiar static pushover analysis. At its core, it involves analyzing a

model under a suite of ground excitation records, scaled to several levels of intensity.

An IDA approach encompasses a wide range of the structure behaviour from its elastic response, the nonlinear range and the dynamic instability. The end results are curves of response described in terms of a scalar Damage Measure (DM) versus ground excitation intensity, often given by a scalar Intensity Measure (IM). DM is an index value that expresses the state of damage resulting from a given demand and IM characterizes the hazard. DM is usually defined based on an Engineering Demand Parameter (EDP) such as the drift, plastic rotation, etc. in the structure. Essentially, one can derive the distribution of DM given the IM level as a fundamental element of Performance-Based Earthquake Engineering (PBEE).

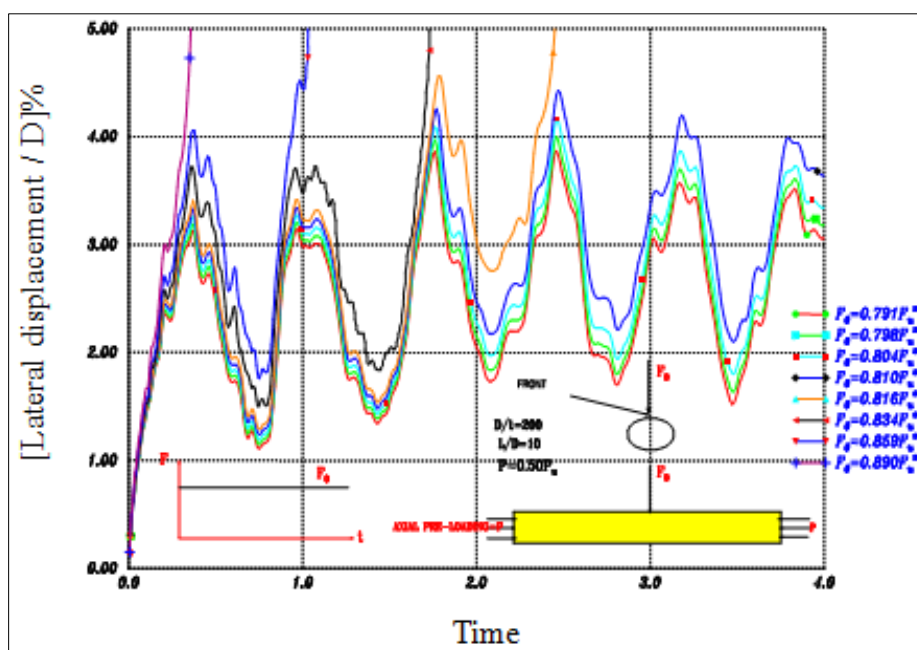


Fig. 10: Time History of the Front Side Displacement for an Axially Pre-Compressed Tube under Incremental Dynamic Lateral Impact Loads [25].

Given a structure and a ground excitation, IDA is performed by conducting a series of nonlinear time-history analyses. The intensity of the ground excitation, defined using an IM, is incrementally increased in each analysis. An EDP, such as global drift ratio, is monitored during each analysis. The extreme values of a DM are identified and plotted against the

corresponding value of the ground excitation IM for each intensity level to produce a dynamic pushover curve for the structure and the chosen earthquake record (see Figure 11). The resulting DMs are later evaluated against that specific Engineering Demand Parameter (EDP).

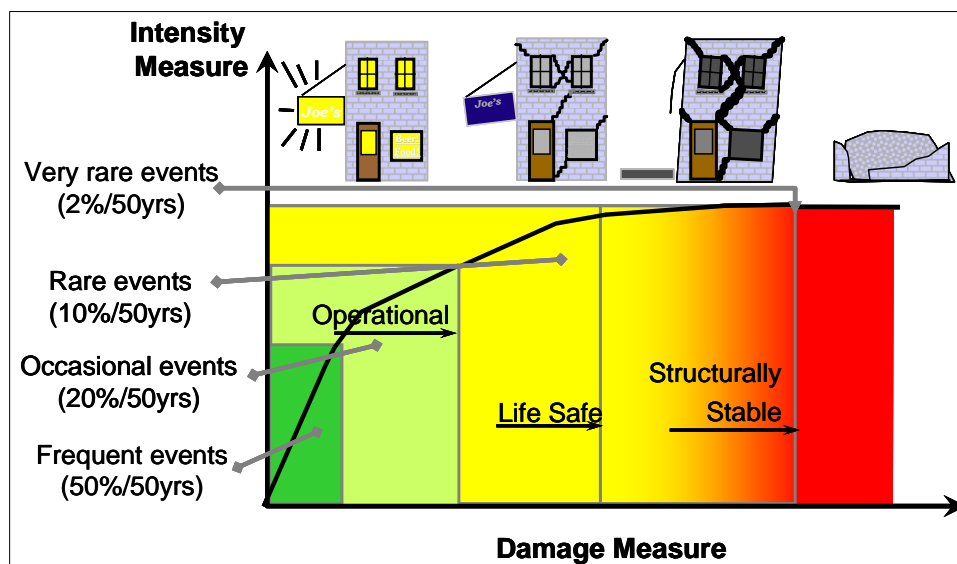


Fig. 11: Anatomy of an IDA Curve in Conjunction with Various Behaviour of the Structure [27].

RESULTS AND DISCUSSIONS

The structure has been excited using acceleration records of far and near-source earthquakes listed in Table 3. Each accelerogram has been incrementally scaled up and down to represent incremental Intensity Measures (IM). Each of these scaled accelerograms has been separately introduced to the platform model.

The maximum inter-storey drift has been considered as the Engineering Demand Parameter (EDP). In each case, all inter-storey drift ratios have been monitored throughout the response time history.

The maximum inter-storey drift ratio all along the jacket structure has been identified as the Damage Measure (DM) with that particular Intensity Measure (IM). These two will represent one point in the IDA graph. This procedure has been repeated for all other intensity measures for a specific earthquake record. Then this has been carried out once again for other near and far-source records listed in Table 3. Figure 12 shows, as an

example, the response of the jacket platform to incrementally scale up near-source records from the Kobe 1995 earthquake. The figure presents the time history of the topside drift under three different intensity measures. As it can be noticed under certain levels of intensity measure the jacket might experience inelastic behaviour but the response remains bounded. Beyond certain intensity measures the response becomes unbounded.

This behaviour can be used to appreciate whether, under a specific dynamic excitation, the numerical system has experienced a dynamic instability or remained stable. With an implicit direct integration numerical approach, if the response of a structure to a dynamic excitation is bounded, this indicates that the excited structure remains stable and no global failure occurs. An unbounded response indicates the propagation of dynamic instability in the system. It should be noted that for a MDOF system, an exact solution for the dynamic limit point load does not exist. Only Minimum Guaranteed Critical Loads (MGCL) can be evaluated [24,28,29].

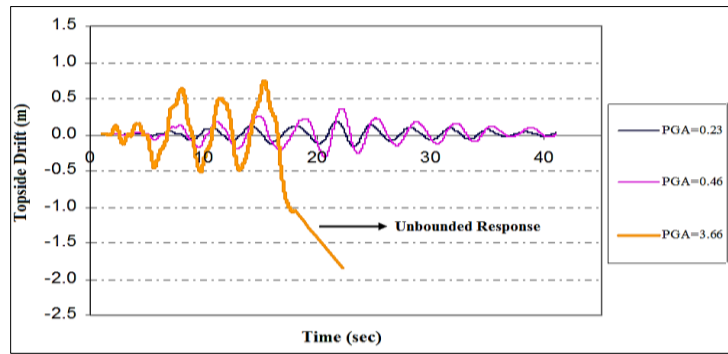


Fig. 12: The Response of SP2 to an Incrementally Scaled up Near-Source Kobe 1995 Earthquake Record.

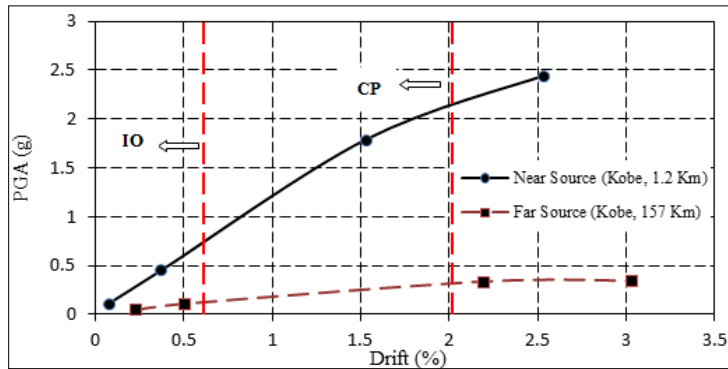


Fig. 13: The IDA Curves for the SP2 Under Far and Near-Source Kobe 1995 Earthquake Excitations.

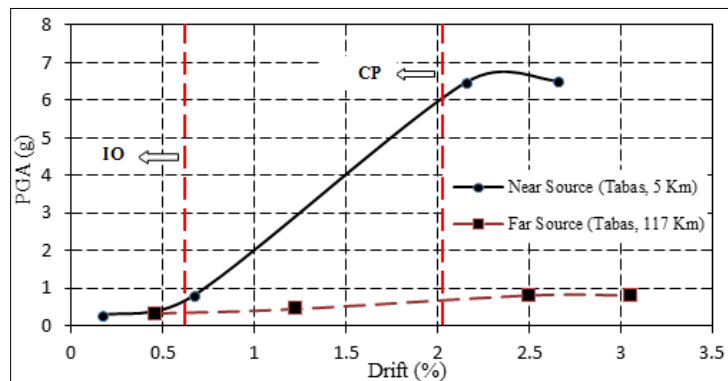


Fig. 14: The IDA Curves for the SP2 Under Far and Near-Source Tabas 1978 Earthquake Excitations.

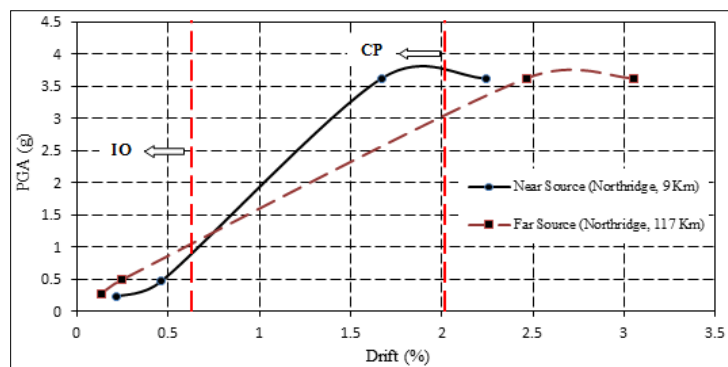


Fig. 15: The IDA Curves for the SP2 Under Far and Near-Source Northridge, 1994 Earthquake Excitations.

Figures 13 and 14, present the IDA graphs for the far and near-source Kobe 1995 and Tabas 1978 excitations, respectively.

The ordinate in these figures, gives the intensity measure as in the form of PGA for the scaled accelerograms while the abscissa shows the damage measure in the form of the maximum inter-storey drift ratio all along the platform stories. It should be noted that each IDA graph is output of many time domains nonlinear dynamic analysis. Generally speaking, in an IDA graph the lowest curve, in respect to the ordinate, represents the highest level of the structural demand, so can be regarded as the most critical type of the excitation to the structure. Accordingly and as an example, Figures 13 and 14 indicate that the Kobe and Tabas far-source excitations have been more critical to the structure than their corresponding near-source earthquakes. As the IDA curves do not often overlay each other and may intersect one another (e.g. Figure 15 for the Northridge, 1994 earthquake). The best practice, so, will be to assess the results against predefined structural performance targets.

PERFORMANCE TARGETS

The Northridge (1994), Kobe (1995) and Chi-Chi (1999) earthquakes supported the idea that the large displacement demand of near-source ground excitations, due to inherent pulse-like waveforms, could not be accommodated by structures proportioned to fulfill requirements of traditional force-based design (FBD).

Current trends in the development of future building codes have all embraced the concept of performance based design (PBSD) in which the structural performance is described by the earthquake-induced displacements through the implementation of displacement-based design (DBD) procedures [30]. In the current study in order to seismic performance evaluate of the jacket type structures, the IDA results for the near and far-source earthquakes have also been examined against two respective target performance levels.

These are the Immediate Occupancy (IO) and Collapse Prevention (CP) performance levels, in accordance with FEMA 356 [31]. The current practices for the seismic design of a

jacket platform based on API RP 2A [32] and ISO 19901-2 [33], is to analyses the structure against two strength and ductility level earthquakes (or Extreme Level Earthquake and Abnormal Level Earthquake as per ISO 19901-2). The structure should remain elastic under a strength level earthquake. Inelastic behavior and structural damage may occur under a ductility level earthquake but structure collapse shall be avoided.

In fact, the above mentioned criterion of pure elastic response during a strength level earthquake is more restrictive than an IO performance level. The CP performance level, however, appears analogous to the ductility level criteria.

In the current study, the maximum drift ratio of the jacket stories has been considered as the Engineering Demand Parameter (EDP). Limits of 0.6% and 2% maximum storey drift ratio have been assumed for the IO and CP performance levels. For important and tall buildings (taller than 50m), the Iranian code of practice for the seismic design of building defines a maximum of 0.5% for the storey drift ratio or the global drift ratio [34]. This seismic code is principally aimed on minimizing the life risk. The Life Safety (LS) performance level lies somewhere between IO and CP (see Figure 16). Since a jacket structure appears less drift sensitive as compared to buildings, the above selected IO and CP limits looks justifiable. Currently not specific and generally accepted seismic performance targets, similar to those set forward by FEMA 356 for buildings, has been defined for jacket platforms and the subject needs to be separately investigated.

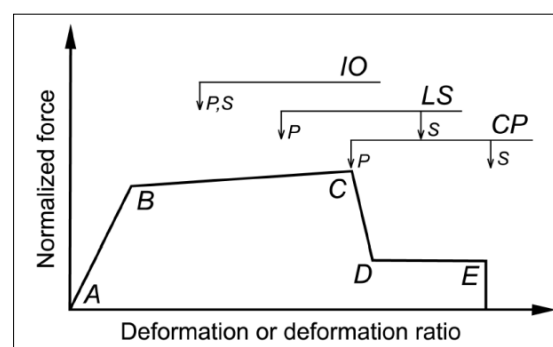


Fig. 16: Generalized Component Force-Deformation Relations for Acceptance Criteria [31].

In accordance with above discussions about the performance targets and for the structure studied, the Kobe and Tabas far-source excitations seem to require higher structural demands under both IO and CP performance targets as compared to their corresponding near-source earthquakes (Figures 13 and 14). For the Northridge earthquake, the structure exhibits a more favorable response to the near-source earthquake under an IO target. Under a CP performance target once again the far-source earthquake has become the governing excitation.

It should be mentioned that the pulse recorded during Tabas, Iran September 16, 1978, 7.4 magnitude earthquake is one of the most distinctive pulses in the database, with a duration of 4.5 seconds. Unique to this pulse is the location of the pulse within the record. The typical pulse occurs at the beginning of the record. This pulse has a peak velocity of 1.21m/s [15].

The pulse for the Kobe (1995) and Northridge (1994) near-source records in Table 3 has the duration of 1.3s and 1.1s, and a peak velocity of 0.74m/s and 0.85m/s, respectively. For the jacket platform studied (and at least at an IO performance target), the Northridge record near-source appeared to be the most critical amongst other near-source records. This is while the pulse with Tabas near-source record has the highest peak velocity and duration. This seems because at an IO performance target the structure still remains close to its elastic range with a natural period around 1.49s.

The Tabas pulse duration is far away from the structure's natural period of vibration. This is while the pulse duration in Northridge record is closer to the natural period. So at the IO target the Northridge near-source record has become critical. At the CP target, however, the far-source record appears more unfavorable. This is likely because next to a CP target, the structure undergoes extensive inelastic deformations.

The structure stiffness so decreases and its natural period will increase. As a result, the natural period of the structure moves away

from the pulse duration and once again the far-source excitation becomes more critical.

It should be mentioned that the records listed in Table 3 have been also introduced into the model for the SP2 platform. The same IDA approach has been used and similar results have been obtained for the response of the P3D platform against the far and near-source earthquakes. For this platform, however, the far-source excitations have been found to be more critical than those from the near-source records.

CONCLUSION

In this paper, models of two operating fixed jacket platform in the Persian Gulf have been numerically studied against different far and near source earthquake excitations. A time domain dynamic direct integration approach, accounting for the structure geometrical and material nonlinearities and the soil/pile inelastic dynamic interactions, has been chosen for the study. The numerical model has been verified against experimental results for the cyclic loading of tubular frames from other researchers.

The selected ground excitation records have all magnitudes above 6.7 and are from those earthquakes which both their far and near-source records are available. All selected near-source records contain relatively large directivity velocity pulses. To get an insight into both the pre and post failure zones of the structure response, an incremental dynamic analysis approach has been employed. Several performance targets have also been discussed to ease the assessment of the platform response to dynamic ground excitations. In general, it has been found that with some jacket models the near-source excitations appear to be critical as compared with those from the corresponding far-sources. With some models, however, the far-source excitations have been found to be more unfavorable. Prevalently, it has been noticed that the correspondence between the pulse duration, the pulse peak velocity and the main natural frequency of the jacket structure can be used as a criterion to prejudge whether far or the near-source earthquakes are critical for a certain jacket structure.

REFERENCES

1. Kayvani K, Barzegar F. Hysteretic modeling of tubular members and offshore platforms. *Engineering Structures*. 1996; 18(2): 93-101.
2. Conte JP, Peng BF. Fully non-stationary analytical earthquake ground-motion model. *Engineering Mechanics*. 1997; 123(1):15-25.
3. Peng BF, Chang B, Llorente C. Nonlinear dynamic soil-pile-structure interaction analysis of a deep-water platform for ductility level earthquakes. *Proceeding of the Offshore Technology Conference (OTC)*; Huston, Texas 2005.
4. Golafshani AA, Tabeshpour MR, Komaci Y. FEMA approach in seismic assessment of jacket platforms (case study: Ressalat jacket of Persian Gulf). *Constructional Steel Research*. 2009; 65 (10-11): Pages: 1979-1986.
5. Moustafa A, Takewaki I. Deterministic and probabilistic representation of near-field pulse-like ground motion. *Soil Dynamics and Earthquake Engineering*. 2010; 30(5): 412-422.
6. Somerville P. Characterizing near fault ground motion for the design and evaluation of bridges. *Proceeding of third national seismic conference and workshop on bridges and highways*; Portland, Oregon; 2002.
7. Akkose M, Simsek E. Non-linear seismic response of concrete gravity dams to near-fault ground motions including dam-water-sediment-foundation interaction. *Applied Mathematical Modelling*. 2010; 34(11): 3685-3700.
8. Dutta SC, Bhattacharya K, Roy R. Response of low-rise buildings under seismic ground excitation. *Soil Dynamics and Earthquake Engineering*. 2004; 24(12): 893-914.
9. Jalali R, Trifunac MD, Ghodrati G, Zahedi M. Wave-passage effects on strength-reduction factors for design of structures near earthquake faults. *Soil Dynamics and Earthquake Engineering*. 2007; 27(8): 703-711.
10. Zeinoddini M, Matin Nikoo H, Ahmadpour F. A couple soil-fluid-structure simulation of the near-field earthquake effects on gravity type quay-walls. *China Ocean Engineering*. 2013; 27(4): 481-494.
11. Tang Y, Zhang J. Response spectrum-oriented pulse identification and magnitude scaling of forward directivity pulses in near-fault ground motions. *Soil Dynamics and Earthquake Engineering*, 2011; 31(1): 59-76.
12. GB50011-2001. National standards of the people's republic of China, code for seismic design of buildings, *Department of Standards and Norms Ministry of Construction of the People's Republic of China*. 2001.
13. Stewart JP, Chiou SJ, Bray JD, Graves RW, et al. Ground motion evaluation procedures for performance-based design. *Pacific Earthquake Engineering Research Center; Report No. PEER-2001/09*, University Of California, Berkeley, 2001.
14. ICBO, International Conference of Building Officials. Uniform Building Code, UBC 1997 Edition, California, CA. 1997.
15. Cox KE, Ashford SA. Characterization of large velocity pulses for laboratory testing. *Pacific Earthquake Engineering Research Center; Report No Report 2002/22*, University Of California, Berkeley, 2002.
16. Abrahamson NA. Effects of rupture directivity on probabilistic seismic hazard analysis. *Proceedings of the 6th International Conference on Seismic Zonation (6ICSZ)*, Palm Springs, CA, 2000.
17. Tirca L, Foti D, Diaferio M. Response of middle-rise steel frames with and without passive dampers to near-field ground motions. *Engineering Structures*. 2003; 25(2): 169-179.
18. Agrawal AK, He WL. A closed-form approximation of near-fault ground motion pulses for flexible structures. *Proceeding of 15th ASCE Engineering Mechanics Conference*, Columbia University, New York, 2002.
19. SIMULIA, ABAQUS analysis and theory manuals. *The Dassault Systèmes, Realistic Simulation*, Providence, USA. 2007.
20. Clough RW, Penzien J. *Dynamics of structures*. Second Edition, McGraw-Hill Inc. 1993.

21. Bathe KJ. *Finite element procedure in engineering analysis*. Prentice-Hall Inc, 2nd Edition. 1996.
22. Bolt HM, Billington K, Ward K. Results from large scale ultimate load tests on tubular jacket structures. *Proceeding of the Offshore Technology Conference (OTC)*, Houston, Texas, 1994.
23. Nichols NW, Kam JCP, Sharp JV. Benchmarking of collapse analysis of large scale ultimate load tests on tubular jacket frame structure. *International Conference on Offshore Structural Design-Hazards, Safety and Engineering*, London, 1994: 2.2.1-2.2.29.
24. Zeinoddini M, Harding JE, Parke GAR. Dynamic behaviour of axially Pre-loaded tubular steel member of offshore structures subjected to impact damage. *Ocean Engineering*. 1999; 26(10): 963-978.
25. Zeinoddini M, Harding JE, Parke GAR. Interface forces in laterally impacted steel tubes. *Experimental Mechanics*. 2008; 48(3): 265-280.
26. Vamvatsikos D, Cornell CA. Incremental dynamic analysis. *Earthquake Engineering and Structural Dynamics*. 2002; 31(3):491-514.
27. Hamburger RO, Moehle JP. State of performance-based engineering in the United States. *Proceedings of the Second US-Japan Workshop on Performance-Based Design Methodology for Reinforced Concrete Building Structures*. Sapporo, Japan, 2000.
28. Simitises GJ. Dynamic stability of suddenly loaded structures. Springer-Verlag, New York Inc. 1990.
29. Zeinoddini M, Harding JE, Parke GAR. Axially pre-loaded steel tubes subjected to lateral impacts (a numerical simulation). *Impact Engineering*. 2008; 35(11): 1267-1279.
30. Gülkan P, Akkar S. A simple replacement for the drift spectrum. *Engineering Structures*. 2002; 24(11): 1477-1484.
31. FEMA 356. Handbook for the seismic evaluation of buildings-a pre-standard. Washington, D.C. 2000.
32. American Petroleum Institute (API RP 2A-WSD). Recommended practice for planning, designing and constructing fixed offshore platforms. 2000.
33. International Organization for Standardization. ISO 19902-Petroleum and natural gas industries-fixed steel offshore structures. DIS version, 2004.
34. BHRC No.S-253. Iranian code of practice for seismic resistant design of building. Standard 2800- 3rd Edition, 2006.